Stoelben E, Petersen I, Clement JH, Sänger J, Muscarella LA, la Torre A, Fazio VM, Lahortiga I, Perera T, Ogata S, Parade M, Brehmer D, Vingron M, Heukamp LC, Buettner R, Zander T, Wolf J, Perner S, Ansén S, Haas SA, Yatabe Y, Thomas RK. CD74-NRG1 fusions in lung adenocarcinoma. *Cancer Discovery*. 4: 415-22, 2014.

3. Fukatsu A, Ishiguro F, Tanaka I, Kudo T, Nakagawa K, Shinjo K, Kondo Y, Fujii M, Hasegawa Y, Tomizawa K, Mitsudomi T, Osada H, Hata Y, Sekido Y. RASSF3 downregulation increases malignant phenotypes of non-small cell lung cancer. *Lung Cancer*. 83: 23-9, 2014.
4. Okamoto Y, Shinjo K, Shimizu Y, Sano T, Yamao K, Gao W, Fujii M, Osada H, Sekido Y, Murakami S, Tanaka Y, Joh T, Sato S, Takahashi S, Wakita T, Zhu J, Issa JP, Kondo Y. Hepatitis virus infection affects DNA methylation in mice with humanized livers. *Gastroenterology*. 146: 562-72, 2014.

2）学会発表

1. Osada H, Yanagisawa K, Tatematsu Y, Sekido Y, Takahashi T. CRISPR-Cas9-derived Knockout of CLCP1 gene revealed its functional role in lung cancer progression. 第 73 回日本癌学会学術総会(口演)、横浜、2014 年 9 月 25-27 日.
2. 長田啓隆、柳澤聖、立松義朗、谷田部恭、小野健一郎、関戸好孝、高橋隆。Genome editing を用いた転移関連遺伝子 CLCP1 の機能解析。第 37 回日本分子生物学会年会(ポスター)、横浜、2014 年 11 月 25-27 日

G．知的財産権の出願・登録状況

1. 特許取得
   なし

2. 実用新案登録
   なし

3. その他
   なし

III. 学会等発表実績

様式第19

学 会 等 発 表 実 績

委託業務題目
「クリニカルプロテオミクス解析を基盤とする肺がんの分子病態の解明と革新的分子標的治療の開発」

機関名　名古屋大学

1. 学会等における口頭・ポスター発表

発表した成果(発表題目、口頭・ポスター発表の別)	発表者氏名	発表した場所(学会等名)	発表した時期	国内・外の別
ROR1, a transcriptional target of TTF-1/NKX2-1 oncogene, sustains lineage-survival signaling in lung adenocarcinoma.	Takahashi T	Berlin (Japanese-German Workshop)	2014年11月	国外
Proteomic analyses for biomarker discovery in human pancreatic cancer. (ポスター)	Yanagisawa K, Kawahara T, Ozawa Y, Hotta N, Nagino M, Takahashi T	Madrid, Spain (13th Annual World Congress of the Human Proteome Organization)	2014年10月	国外
Elucidation of transcriptional regulatory circuitry involved in the molecular pathogenesis of lung cancer. (口頭)	Takahashi T	横浜 (第73回日本癌学会学術総会)	2014年9月	国内
CKAP4 confers resistance to amino acid insufficiency through sequestration of GCN2 in malignant pulmonary mesothelioma. (口頭)	Yanagisawa K, Kato S, Hotta N, Nakamura S, and Takahashi T	横浜 (第73回日本癌学会学術総会)	2014年9月	国内
CRISPR-Cas9-derived Knockout of CLCP1 gene revealed its functional role in lung cancer progression. (口頭)	Osada H, Yanagisawa K, Tatematsu Y, Sekido Y, Takahashi T	横浜 (第73回 日本癌学会学術総会)	2014年 9月	国内
Genome editingを用いた転移関連遺伝子CLCP1の機能解析 (ポスター)	長田啓隆、柳澤聖、立松義朗、谷田部恭、小野健一郎、関戸好孝、高橋隆	横浜 (第37回 日本分子生物学会年会)	2014年11月1日	国内

2. 学会誌・雑誌等における論文掲載

掲載した論文(発表題目)	発表者氏名	発表した場所(学会誌・雑誌等名)	発表した時期	国内・外の別
Lung adenocarcinoma subtypes definable by lung development-related miRNA expression profiles in association with clinicopathologic features. Carcinogenesis	Arima C, Kajino T, Tamada Y, Imoto S, Shimada Y, Nakatochi M, Suzuki M, Isomura H, Yatabe Y, Yamaguchi T, Yanagisawa K, Miyano S, Takahashi T.	Carcinogenesis 35: 2224-2231	2014, Oct	国外

Cancer-promoting role of adipocytes in asbestos-induced mesothelial carcinogenesis through dysregulated adipocytokine production.	Chew SH, Okazaki Y, Nagai H, Misawa N, Akatsuka S, Yamashita K, Jiang L, Yamashita Y, Noguchi M, Hosoda K, Sekido Y, Takahashi T, Toyokuni S.	Carcinogenesis 35: 164-172	2014, Jul	国外
Connective tissue growth factor and β-catenin constitute an autocrine loop for activation in rat sarcomatoid mesothelioma.	Jiang L, Yamashita Y, Chew SH, Akatsuka S, Ukai S, Wang S, Nagai H, Okazaki Y, Takahashi T, Toyokuni S.	J. Pathol. 233: 402-414	2014, Aug	国外
Expression of chromobox homolog 7 (CBX7) is associated with poor prognosis in ovarian clear cell adenocarcinoma via TRAIL-induced apoptotic pathway regulation.	Shinjo K, Yamashita Y, Yamamoto E, Akatsuka S, Uno N, Kamiya A, Niimi K, Sakaguchi Y, Nagasaka T, Takahashi T, Shibata K, Kajiyama H, Kikkawa F, Toyokuni S.	Int. J. Cancer 135: 308-318,	2014, Jul	国外
Neurotensin (NTS) and its receptor (NTSR1) causes EGFR, HER2 and HER3 over-expression and their autocrine/paracrine activation in lung tumors, confirming responsiveness to erlotinib.	Younes M, Wu Z, Dupouy S, Lupo AM, Mourra N, Takahashi T, Flejou JF, Tredaniel J, Regnard JF, Damotte D, Alifano M, Forgez P.	Oncotarget 5: 8252-8269	2014, Sep	国外
Tumor-derived Interleukin-1 promotes lymphangiogenesis and lymph node metastasis through M2-type macrophages.	Watari K, Shibata T, Kawahara A, Sata K, Nabeshima H, Shinoda A, Abe H, Azuma K, Murakami Y, Izumi, H, Takahashi T, Kage M, Kuwano M, Ono M.	PLoS ONE 9: e999568	2014, Jun	国外

様式第19

学 会 等 発 表 実 績

委託業務題目
「クリニカルプロテオミクス解析を基盤とする肺がんの分子病態の解明と革新的分子標的治療の開発」

機関名　愛知県がんセンター研究所

1. 学会等における口頭・ポスター発表

発表した成果(発表題目、口頭・ポスター発表の別)	発表者氏名	発表した場所(学会等名)	発表した時期	国内・外の別
CRISPR-Cas9-derived Knockout of CLCP1 gene revealed its functional role in lung cancer progression. (口頭)	Osada H, Yanagisawa K, Tatematsu Y, Sekido Y, Takahashi T	横浜 (第73回 日本癌学会学術総会)	2014年 9月	国内
Genome editingを用いた転移関連遺伝子CLCP1の機能解析 (ポスター)	長田啓隆、柳澤聖、立松義朗、谷田部恭、小野健一郎、関戸好孝、高橋隆	横浜 (第37回 日本分子生物学会年会)	2014年11月1日	国内

2. 学会誌・雑誌等における論文掲載

掲載した論文(発表題目)	発表者氏名	発表した場所(学会誌・雑誌等名)	発表した時期	国内・外の別
LIM-domain protein AJUBA suppresses malignant mesothelioma cell proliferation via Hippo signaling cascade.	Tanaka I, Osada H, Fujii M, Fukatsu A, Hida T, Horio Y, Kondo Y, Sato A, Hasegawa Y, Tsujimura T, Sekido Y.	Oncogene 34: 73-83	2015, Jan	国外
CD74-NRG1 fusions in lung adenocarcinoma.	Fernandez-Cuesta L, Plenker D, Osada H, Sun R, Menon R, Leenders F, Ortiz-Cuaran S, Peifer M, Bos M, Daßler J, Malchers F, Schöttle J, Vogel W, Dahmen I, Koker M, Ullrich RT, Wright GM, Russell PA, Wainer Z, Solomon B, Brambilla E, Nagy-Mignotte H, Moro-Sibilot D, Brambilla CG, Lantuejoul S, Altmüller J, Becker C, Nürnberg P, Heuckmann JM, Stoelben E, Petersen I, Clement JH, Sänger J, Muscarella LA, la Torre A, Fazio VM, Lahortiga I, Perera T, Ogata S, Parade M, Brehmer D, Vingron M, Heukamp LC, Buettner R, Zander T, Wolf J, Perner S, Ansén S, Haas SA, Yatabe Y, Thomas RK.	Cancer Discovery. 4: 415-422	2014, Apr	国外

RASSF3 downregulation increases malignant phenotypes of non-small cell lung cancer.	Fukatsu A, Ishiguro F, Tanaka I, Kudo T, Nakagawa K, Shinjo K, Kondo Y, Fujii M, Hasegawa Y, Tomizawa K, Mitsudomi T, Osada H, Hata Y, Sekido Y.	Lung Cancer. 83: 23-29	2014, Jan	国外
Hepatitis virus infection affects DNA methylation in mice with humanized livers.	Okamoto Y, Shinjo K, Shimizu Y, Sano T, Yamao K, Gao W, Fujii M, Osada H, Sekido Y, Murakami S, Tanaka Y, Joh T, Sato S, Takahashi S, Wakita T, Zhu J, Issa JP, Kondo Y.	Gastroenterology. 146: 562-572	2014, Feb	国外

Ⅳ．研究成果の刊行物・別刷

Carcinogenesis vol.35 no.10 pp.2224–2231, 2014
doi:10.1093/carcin/bgu127
Advance Access publication June 5, 2014

Lung adenocarcinoma subtypes definable by lung development-related miRNA expression profiles in association with clinicopathologic features

Chinatsu Arima†, Taisuke Kajino†, Yoshinori Tamada[1,†], Seiya Imoto[1], Yukako Shimada, Masahiro Nakatochi[2], Motoshi Suzuki, Hisanori Isomura, Yasushi Yatabe[3], Tomoya Yamaguchi, Kiyoshi Yanagisawa, Satoru Miyano[1] and Takashi Takahashi*

Division of Molecular Carcinogenesis, Center for Neurological Diseases and Cancer, Nagoya University Graduate School of Medicine, Nagoya 466-8550, Japan, [1]Laboratory of DNA Information Analysis, Human Genome Center, Institute of Medical Science, University of Tokyo, Tokyo 108-8639, Japan, [2]Center for Advanced Medicine and Clinical Research, Nagoya University Hospital, Nagoya 466-8550, Japan and [3]Department of Pathology and Molecular Diagnostics, Aichi Cancer Center Hospital, Nagoya 464-8681, Japan

*To whom correspondence should be addressed. Tel: +81 52 744 2454; Fax: +81 52 744 2457;
Email: tak@med.nagoya-u.ac.jp

Accumulation of genetic and epigenetic changes alters regulation of a web of interconnected genes including microRNAs (miRNAs), which confer hallmark capabilities and characteristic cancer features. In this study, the miRNA and messenger RNA expression profiles of 126 non-small cell lung cancer specimens were analyzed, with special attention given to the diversity of lung adenocarcinomas. Of those, 76 adenocarcinomas were classified into two major subtypes, developing lung-like and adult lung-like, based on their distinctive miRNA expression profiles resembling those of either developing or adult lungs, respectively. A systems biology-based approach using a Bayesian network and non-parametric regression was employed to estimate the gene regulatory circuitry functioning in patient tumors in order to identify subnetworks enriched for genes with differential expression between the two major subtypes. *miR-30d* and *miR-195*, identified as hub genes in such subnetworks, had lower levels of expression in the developing lung-like subtype, whereas introduction of *miR-30d* or *miR-195* into the lung cancer cell lines evoked shifts of messenger RNA expression profiles toward the adult lung-like subtype. Conversely, the influence of *miR-30d* and *miR-195* was significantly different between the developing lung-like and adult lung-like subtypes in our analysis of the patient data set. In addition, *RRM2*, a child gene of the *miR-30d*-centered subnetwork, was found to be a direct target of *miR-30d*. Together, our findings reveal the existence of two miRNA expression profile-defined lung adenocarcinoma subtypes with distinctive clinicopathologic features and also suggest the usefulness of a systems biology-based approach to gain insight into the altered regulatory circuitry involved in cancer development.

Introduction

Lung cancer has long been the leading cause of cancer-related deaths worldwide; thus, a better understanding of the molecular pathogenesis of this fatal disease is keenly awaited to reduce the intolerable death toll. Adenocarcinomas arising from peripheral lung tissues are the most frequent histological type and exhibit the highest degree of diversity among various types of lung cancers (1). The TTF-1 transcription factor, a master regulator of peripheral lung development, is expressed in a series of peripheral lung epithelial cells belonging to a distinct cellular lineage, i.e. 'terminal respiratory unit (TRU)', and has also been shown to play a role as a lineage-survival oncogene of lung adenocarcinoma (2–4). Our previous studies demonstrated the existence of two major types of lung adenocarcinomas, i.e. TRU and non-TRU types (3,5). A TRU-type adenocarcinoma characteristically retains features of TRU cells to a certain extent and exhibits uniform and abundant TTF-1 expression as well as distinct messenger RNA (mRNA) expression profiles in association with a high prevalence of epidermal growth factor receptor mutations, female gender and non-smoking status (3,5,6).

Lung cancers carry various genetic and epigenetic alterations in cancer-related, protein-coding genes (7,8), while accumulated evidence also indicates that microRNAs (miRNAs) are involved in lung cancer development (9). We reported previously that *let-7* plays a role as a tumor suppressor miRNA in lung cancers and showed frequent downregulation in association with poor postoperative prognosis (10), whereas the oncogenic miRNA (oncomiR) *miR-17–92* is frequently overexpressed with occasional gene amplification, rendering lung cancer cells addicted to continued expression for cell survival (11–14). It is interesting to note that close relationships of both *let-7* and *miR-17–92* with development and proliferation have been demonstrated, suggesting a possible mechanistic link between altered miRNA expression and cancer development (15,16).

Accumulation of multiple genetic and epigenetic alterations in the cancer genome affects regulation of a web of interconnected genes including miRNAs. The resultant global changes in expression of both protein-coding genes and miRNAs establish a molecular basis for acquisition of hallmark capabilities and characteristic features of cancer cells (17). Although information regarding intergene regulatory relationships and their cascades is steadily accumulating, the entire picture of the gene regulatory circuitry remains elusive, especially regarding its operation in tumor tissues of cancer patients. Along this line, there is expectation that a cancer systems biology approach will help to reveal a path to resolve this challenge with the aid of ever-increasing computing power (18).

In this study, we analyzed the global expression profiles of miRNAs together with those of mRNAs in non-small cell lung cancer (NSCLC) tissues, with special attention given to the diversity of lung adenocarcinomas. We also employed a systems biology-based approach in order to identify the gene regulatory circuitry, which is distinctively involved in two major lung adenocarcinoma subtypes that are definable by their miRNA expression profile.

Abbreviations: miRNA, microRNA; mRNA, messenger RNA; NSCLC, non-small cell lung cancer; TRU, terminal respiratory unit.

†These authors contributed equally to this work.

Materials and methods

Tumor samples and cell line

A series of 126 NSCLC cases, comprising 76 adenocarcinomas, 29 squamous cell carcinomas, 15 large cell carcinomas, 4 adenosquamous carcinomas and 2 large cell neuroendocrine carcinomas, which successfully underwent potential curative resection at Aichi Cancer Center, Nagoya, Japan, were investigated. All tumors were histologically categorized according to the IASLC/ATS/ERS classification (1). Approval of the institutional review boards of Nagoya University Graduate School of Medicine and Aichi Cancer Center and written informed consent from the patients were obtained. All tumor specimens were embedded in OCT compound and stored at −80°C. Seventy-six of the adenocarcinoma cases were included in an analysis of the association between miRNA expression profile-defined subtypes and postoperative prognosis. The median follow-up period of the patients was 79 months (range, 1–111 months) when all eligible cases were included and 91 months (63–111 months) after excluding deceased cases. SK-LC-7 and SK-Lu-1, lung adenocarcinoma cell lines, were gifts from late Dr Lloyd J. Old (Memorial Sloan Kettering Cancer Institute) and maintained in RPMI-1640 with 5% fetal bovine serum (19,20). Detailed information regarding their verification is provided in the Supplementary Materials and methods, available at *Carcinogenesis* Online.

Microarray analysis of miRNA and mRNA expression profiles

Frozen tissues from the tumor specimens were subjected to gross microdissection under the guidance of a pathologist (Y.Y.) to ensure at least 50% tumor cell content using every 10th section stained with Giemsa. Total RNA was extracted using an miRNeasy Mini kit (Qiagen), followed by treatment with DNase I. Microarray analysis was conducted to examine miRNA expression profiles using a Human miRNA Microarray (precommercial version, Agilent) with 470 miRNA probes, according to the manufacturer's instructions. Microarray analysis was also conducted to examine the effects of *miR-30d* and *miR-195* on mRNA expression, using Whole Human Genome 4x44K Microarrays (G4112F, Agilent) and a large batch of common reference RNA of a mixture of 20 lung cancer cell lines, as described previously (21). We also utilized our previous data sets of mRNA expression profiles (21) and *EGFR*, *K-ras* and *p53* mutations (5) of the same lung adenocarcinoma sample set, except for a single case. In addition, microarray analysis was newly conducted to acquire mRNA expression profile data for the non-adenocarcinoma samples used in this study, which included 49 NSCLC tumor samples with a histology other than adenocarcinoma (a single squamous cell carcinoma specimen was not available for the additional analysis) and four mixtures of normal lung tissues. All microarray data obtained in this study are available at the Gene Expression Omnibus under the following accession number (GSE51855).

Bioinformatics and systems biology-based analyses

Microarray analysis data of miRNA expression were first log2-transformed and normalized to the 75th percentile, followed by filtering to select miRNAs with expression in at least 10% of the samples. Consequently, 303 miRNAs were selected for subsequent hierarchical clustering analysis of the NSCLC samples and 299 for the adenocarcinoma samples. The CLUSTER program was used to perform average linkage hierarchical clustering, using median centering for normalization and uncentered correlation coefficient, and the results were displayed with the aid of TREEVIEW (http://rana.lbl.gov/EisenSoftware.htm) (22). The Database for Annotation, Visualization and Integrated Discovery (DAVID, http://david.abcc.ncifcrf.gov/home.jsp) was used for pathway analysis along with the Kyoto Encyclopedia of Genes and Genomes with false discovery rate (FDR) <25% set as the significance level. Fisher's exact test was used for comparisons of proportions according to the miRNA expression profile-defined subtypes in hierarchical clustering analysis. The Kaplan–Meier method was used to estimate survival as a function of time and survival differences were analyzed with a log-rank test with $P < 0.05$ set as the significance level. Statistical analyses were performed using Stata software (version 7, StataCorp).

For analysis of the relationship of miRNA expression profile-based subtypes with lung development, we selected 18 and 38 miRNAs corresponding to clusters 5 and 1, respectively, in a previous report by Dong *et al.* (23) (GSE21052), which were most specifically expressed in developing and adult lung-predominant types, respectively. Similarly, we used a data set reported by Dong *et al.* (23) (GSE20954 with use of an Affymetrix GeneChip Mouse Genome 430 2.0 Array) to select mRNAs predominantly expressed in either developing or adult lungs. Among 4414 genes that passed filtering for expression and also corresponded to probes on a Whole Human Genome 4x44K Microarray chip (G4112F, Agilent), 2078 developing lung- and 1778 adult lung-predominant mRNAs were consequently identified and subjected to one-way hierarchical clustering analysis (Supplementary Figure 1, available at *Carcinogenesis* Online). The average *z*-scores of each set of genes in clusters 1 and 2 were calculated and then subjected to box plot analysis. A Wilcoxon rank sum test was used to evaluate statistical significance. Statistical analyses were performed with R software version 3.0.1 (http://www.r-project.org) and the two-sided significance level was set at $P < 0.05$.

The gene regulatory network was estimated using SiGN-BN, a Bayesian network and non-parametric regression-based software package, using a supercomputer at the Human Genome Center, Institute of Medical Science, University of Tokyo (http://sign.hgc.jp/signbn/) (24). SiGN-BN estimates regulatory dependencies between genes as gene networks from gene expression data. We made slight modifications to SiGN-BN in order to reconcile our assumption that miRNAs do not have direct regulatory consequences with other miRNAs (Supplementary Materials and methods, available at *Carcinogenesis* Online). Among 464 mRNAs belonging to an Ingenuity Pathway Analysis category of lung tumor (cancer > lung tumor > lung tumor), and 141 mRNAs belonging to an Ingenuity Pathway Analysis category of respiratory system development and function (development > respiratory system development and function), except for those in its subcategories of development of the nose and diaphragm and related cell lines, we selected those exhibiting more than a 2-fold difference in samples between the 10 and 90% tiles in 124 NSCLCs, for which both miRNA and mRNA expression profiles were available. As a result, 400 mRNAs and 32 miRNAs were selected for network estimation with 0.05 used as the bootstrap threshold. In this study, a gene estimated to be in regulatory relationships with multiple genes was defined as a hub gene and those estimated to have regulatory relationships with a hub gene were called child genes.

Experimental evaluations by introduction of miR-30d *or* miR-195

Pre-miR-30d, Pre-miR-195 and Pre-miR-NC#2 were purchased from Ambion. Each Pre-miR molecule was introduced into 1×10^5 of SK-LC-7 and SK-Lu-1 cells with low *miR-30d* and *miR-195* expression using 1 μl/ml of Lipofectamine RNAiMAX (Invitrogen) according to the instructions of the manufacturer. Cells were harvested 72 h after transfection and subjected to western blotting, flow cytometric and colorimetric analyses, essentially as described previously (25,26). Changes in global mRNA expression were also analyzed by microarray analysis as described above. In addition, influences of *miR-30d* or *miR-195* in patients with an adenocarcinoma were estimated. To this end, we first selected genes with a differential expression of >0.5 either up or down (log2 ratio) in response to miRNA introduction in SK-LC-7, from those included in the network estimation. Consequently, 77 and 118 mRNAs were identified as those affected by *miR-30d* and *miR-195* introduction, respectively. We then defined the influence score for each patient based on the following equation in order to evaluate the concordance of expression of *miR-30d* or *miR-195* with changes in these 77 and 118 mRNAs:

$$\text{Influence score}_j = \frac{1}{n}\sum_{i=1}^{n} z_{ij} s_i, \quad \text{where } s_i = \begin{cases} 1 & \text{if } y_i > 0.5 \\ -1 & \text{if } y_i < -0.5 \end{cases}.$$

The log2-transformed expression values of gene *i*, i.e. 77 for *miR-30d* and 118 for *miR-195*, for patient *j* (x_{ij}) were normalized to the Z-transformed score z_{ij}, in which gene *i* had a mean of $\mu_i = 0$ and standard deviation of $\sigma_i = 1$ for all patients with an adenocarcinoma. *n* is the number of the selected genes. s_i is the sign function of y_i, which is a log2 ratio of expression of gene *i* in miRNA mimics-introduced cells to that in control molecule-introduced cells. Wilcoxon rank sum and Kruskal–Wallis tests were used for comparisons of influence scores between the two clusters and among five subclusters, respectively. Statistical analyses were performed with R software version 3.0.1 and the two-sided significance level was set at $P < 0.05$.

A 2033 bp *RRM2* 3′ untranslated region containing a target site for *miR-30d* was amplified by PCR using primers with the SfiI site and cloned downstream of the luciferase coding sequence in the modified pGL3 vector. The following primers were used to amplify the 3′ untranslated region: forward, 5′-AA AGGCCAG TAGGGCCATGAACTGAAGATGTGCCCTTACTTGG-3′; and reverse, 5′-GGC CCTACTGGC CGAAAC TGACATAAGAACAG-3′. To generate a mutation in the predicted target site, seven nucleotides corresponding to the seed sequence were deleted using a QuikChange site-directed mutagenesis kit (Stratagene). A luciferase assay was performed using the resultant vectors, as described previously (26).

Results

Existence of two major types of lung adenocarcinomas according to miRNA expression profiles

Microarray analysis was performed to analyze the miRNA expression profiles of tumor samples from 126 surgically treated NSCLC patients as well as five sets of RNA mixtures, each of which contained five independent normal lung RNAs (25 samples in total). We first performed unsupervised hierarchical clustering based on the expression of 303 miRNAs with expression detected in at least 10% of the NSCLC samples, in order to gain insight into the diversity of NSCLC in relation to miRNA expression profiles. In contrast to our previous mRNA expression profiling analysis recapitulating the widely used histologic classification of NSCLCs (5), adenocarcinomas were not grouped into a single well-defined cluster (Figure 1A). Instead, they were found not only in a cluster primarily consisting of adenocarcinomas along with normal lung tissues but also in the other major cluster containing an admixture of both adenocarcinomas and other histologic types such as squamous cell carcinomas. We then focused our attention specifically to adenocarcinoma diversity. Hierarchical clustering analysis of 76 lung adenocarcinomas was conducted based on the expression of 299 miRNAs with expression in at least 10% of the adenocarcinoma samples (Figure 1B). Cluster 1 with two subclusters was composed of tumors belonging to the admixture cluster in the analysis of NSCLCs. We found that cluster 1 tumors were significantly associated with a less differentiated state, as well as more prominent invasion and necrosis (Table I). In contrast, the mRNA

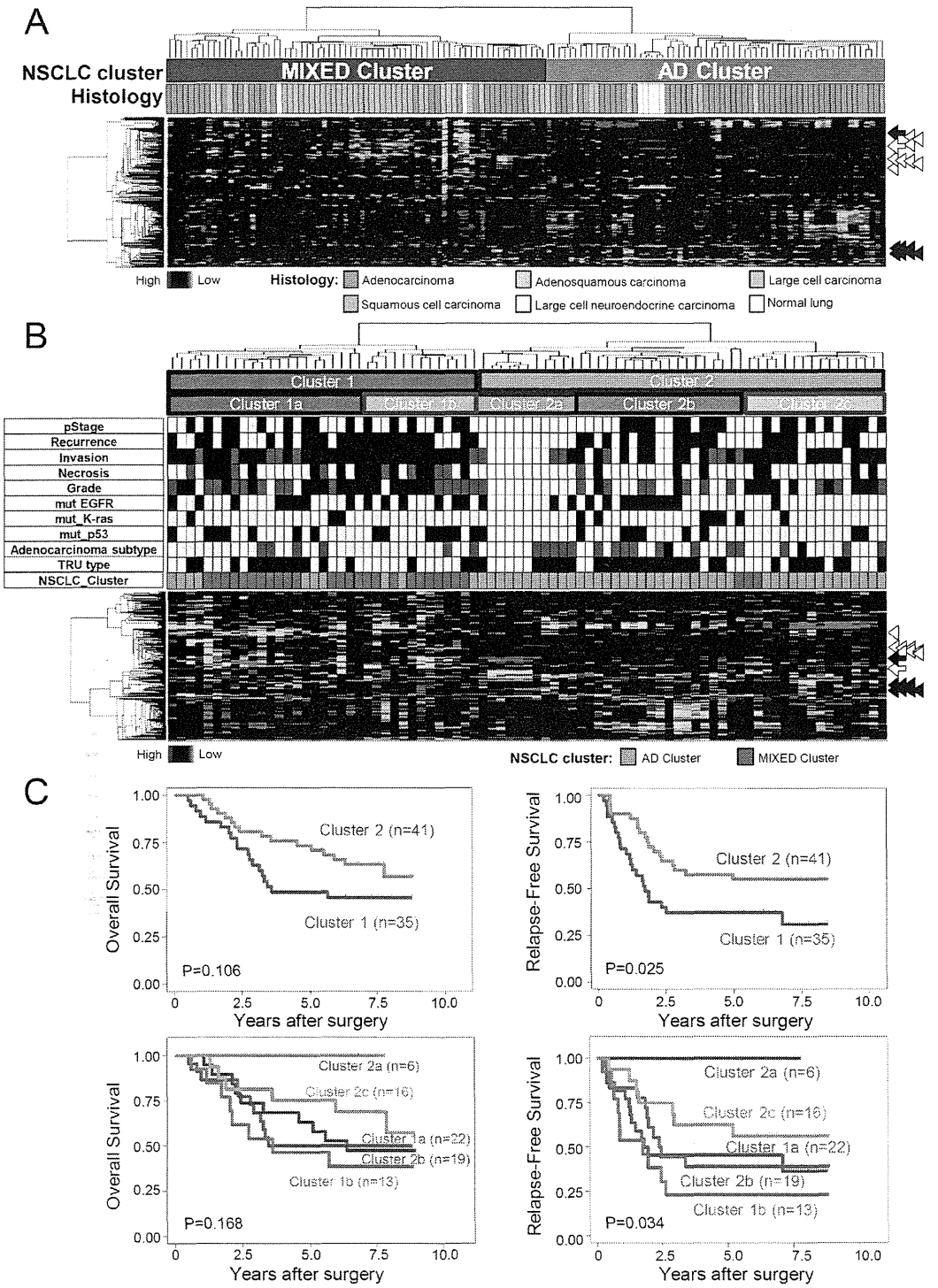

Fig. 1. Expression profiling analysis of lung cancers. Shown are results of hierarchical clustering analysis of (**A**) 126 NSCLCs and (**B**) 76 lung adenocarcinomas. (**C**) Relationship of miRNA expression profile-defined lung adenocarcinoma subtypes with prognosis after surgery. Open arrowheads, *let-7* family; solid arrowheads, *miR-17–92* cluster; open arrow, *miR-30d*; solid arrow, *miR-195*.

expression profile-defined TRU-type classification was significantly more commonly seen in cluster 2 with three subclusters, one of which had expression profiles considerably similar to that of normal lung tissue. Mutations in the *EGFR*, *p53* and *K-ras* genes were not differentially present. Kaplan–Meier survival curves demonstrated significant differences in relapse-free survival among the clusters, whereas no relapse was observed in cluster 2a with expression profiles very similar to that of normal lung tissue. These findings indicated that lung adenocarcinomas can be classified into two major subtypes according to their miRNA expression profiles, showing a distinctive association with clinicopathologic features including postoperative prognosis.

Relationship of two major adenocarcinoma clusters with developmental state of the lung

It is well accepted that miRNAs play important roles in developmental processes (9); thus, we investigated whether miRNA expression

Table I. Relationships of miRNA expression profile-defined adenocarcinoma subtypes with various clinicopathologic and genetic features

Characteristics	Cluster 1	Cluster 2	*P* value[a]
pStage			
Stage II or III	15	18	1.000
Stage I	20	23	
Invasion			
Definite	29	24	0.003
Definite but focal	6	7	
Not obvious or negative	0	10	
Necrosis			
Positive	13	7	0.001
Focal	7	1	
Negative	15	33	
Grade			
Poorly differentiated	17	11	0.003
Moderately differentiated	14	11	
Well differentiated	4	19	
mut_*EGFR*			
Mutant	14	13	0.48
Wild-type	21	28	
mut_*K-ras*			
Mutant	3	7	0.326
Wild-type	32	34	
mut_*p53*			
Mutant	14	9	0.132
Wild-type	21	32	
Adenocarcinoma subtypes			
Adenocarcinoma *in situ*	0	2	0.031
Minimally invasive ADC and lepidic predominant ADC	6	16	
Other subtypes	29	23	
mRNA expression profile-based subtypes			
TRU type	15	28	0.037
Non-TRU type	20	13	

ADC, adenocarcinoma.
[a]Fisher's exact test.

profile-defined subtypes of lung adenocarcinomas may reflect the expression of various miRNAs, which are distinct between developing and adult lungs. To this end, we performed one-way hierarchical clustering analysis according to the expression of 18 miRNAs shown to be predominantly expressed in fetal lung tissues and of 38 predominantly expressed in adult lung tissues (23). A clear difference in lung development-related miRNA expression was readily observed between clusters 1 and 2, as tumor samples belonging to cluster 1 exhibited distinctively high expression of developing lung-predominant miRNAs, whereas those of cluster 2 expressed adult lung-predominant miRNAs at a significantly higher level than seen in cluster 1 (Figure 2A). We also performed one-way hierarchical clustering analysis according to the mRNA expression profiles of a set of protein-coding genes, which we selected based on their predominance in developing and adult mouse lungs (Supplementary Figure 1, available at *Carcinogenesis* Online). As with miRNA expression, developing and adult lung-predominant mRNAs were preferentially expressed at a high level in clusters 1 and 2, respectively (Supplementary Figure 2, available at *Carcinogenesis* Online). These findings supported the notion that the distinctive expression profiles of the two miRNA expression profile-defined subtypes may reflect the regulatory state related to lung development, although the association of cluster 1 with aggressive clinicopathologic features appeared to be consistent with an intrinsic highly proliferative state.

Estimation of gene regulatory circuitry in tumors from lung adenocarcinoma patients

We next attempted to determine the gene regulatory circuitry involving both miRNAs and mRNAs in the two miRNA expression profile-defined subtypes of lung adenocarcinomas. For this, we estimated the genetic network using SiGN-BN software (24) (Figure 3A). We then extracted a subset of the estimated network, which was accordingly composed of subnetworks that were significantly enriched for genes with differential expression between clusters 1 and 2 ($P < 0.001$, with Bonferroni adjustment). As a result, 19 subnetworks along with their hub genes were identified and found to be enriched for genes of

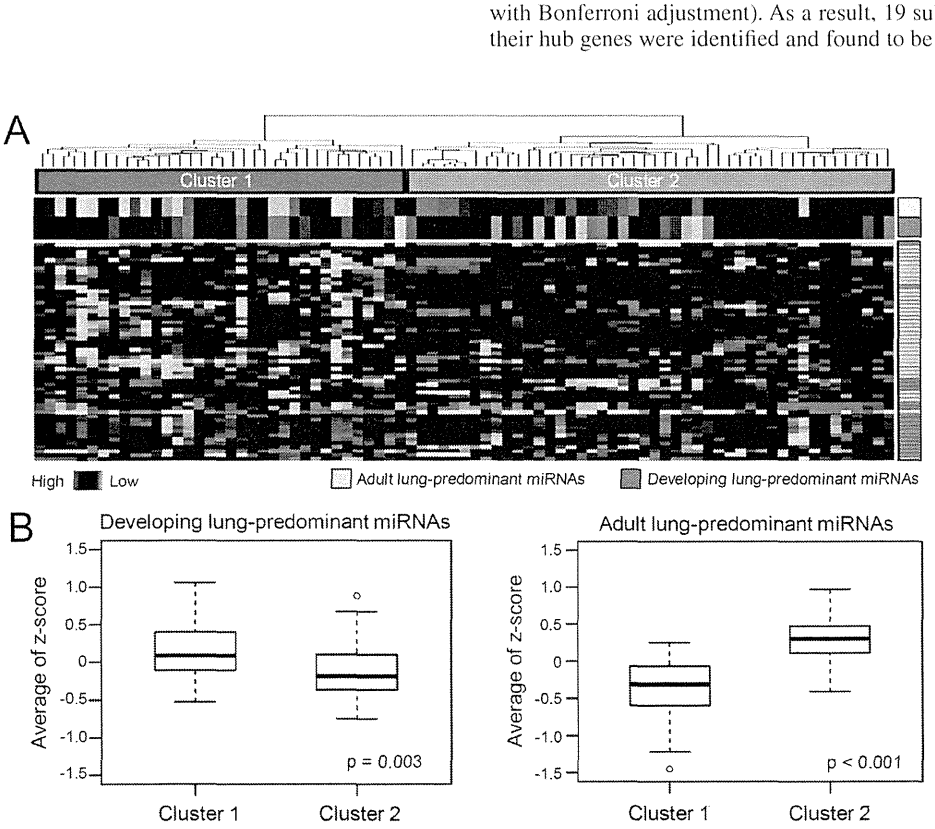

Fig. 2. Hierarchical clustering analysis of lung adenocarcinomas based on (**A**) lung development-related miRNA expression profiles and (**B**) comparisons of average *z*-scores for developing lung- and adult lung-predominant miRNAs between clusters 1 and 2. *P* values calculated using Wilcoxon rank sum test.

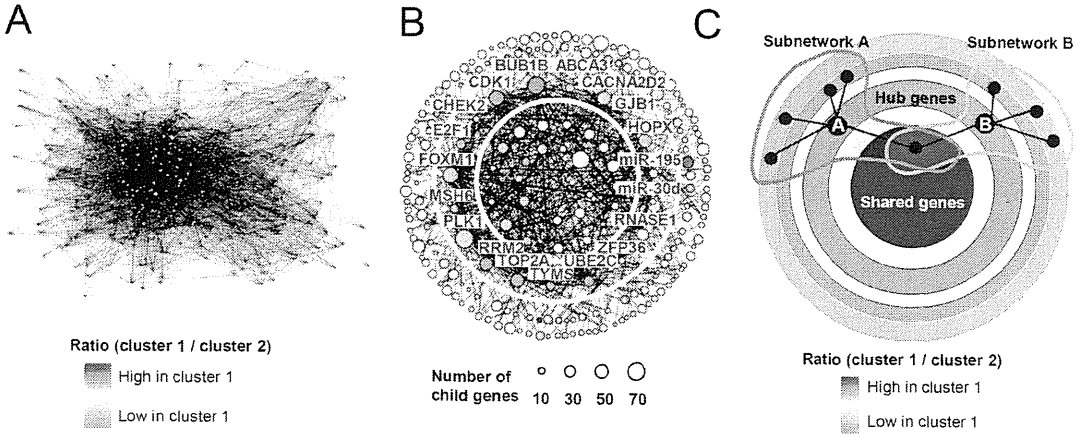

Fig. 3. Estimation of gene regulatory circuitry based on Bayesian network and non-parametric regression using present data set of miRNA expression in tumors from lung cancer patients. (**A**) Results of Bayesian network estimation of regulatory relationships of 400 mRNAs and 32 miRNAs. (**B**) Extracted network harboring 19 subnetworks enriched for genes with differential expression between clusters 1 and 2 (upper panel), and a schematic diagram of subnetworks with hub, child, and shared genes (lower panel). A list of shared core genes, which were frequently shared among the 19 subnetworks, is provided in Supplementary Table 1, available at *Carcinogenesis* Online.

the Kyoto Encyclopedia of Genes and Genomes pathways including cell cycle, nucleic acid metabolism and DNA repair (Figure 3B and Supplementary Table 1, available at *Carcinogenesis* Online). Child genes, which represent those under either direct or indirect regulatory relationships with hub genes, were often shared among the 19 significantly enriched subnetworks (Supplementary Table 2, available at *Carcinogenesis* Online), suggesting their close regulatory relationships.

We also identified two miRNAs, *miR-30d* and *miR-195*, as hub genes of the significantly enriched subnetworks, as they showed lower levels of expression in cluster 1 than in cluster 2. In order to experimentally evaluate the effects of *miR-30d* and *miR-195* on the estimated gene regulatory circuitry, miRNA mimics of *miR-30d* or *miR-195* were transfected into SK-LC-7 cells expressing these miRNAs at a low level. Introduction of these hub miRNAs altered the expression of their child genes in a manner that considerably mimicked their expression in cluster 2 (Figure 4A and 4B). Similar effects were observed in *miR-30d*-transfected SK-Lu-1 cells (Supplementary Figure 3A, available at *Carcinogenesis* Online). It was notable that *miR-30d* markedly decreased *ribonucleotide reductase M2 (RRM2)*, one of the child genes of the *miR-30d*-centered subnetwork and a predicted target for *miR-30d*, as shown by the TargetScan program. Also, western blotting analysis clearly showed downregulation of RRM2 in response to treatment with *miR-30d* mimics in SK-LC-7 and SK-Lu-1 cells (Figure 4C and Supplementary Figure 3B, available at *Carcinogenesis* Online), whereas introduction of *miR-30d* significantly altered cell cycle distribution, resulting in an increase in the G_1 phase and a decrease in S (Figure 4D), as well as inhibition of cell proliferation (Figure 4E and Supplementary Figure 3C, available at *Carcinogenesis* Online). Direct repression of *RRM2* by *miR-30d* via its binding to the predicted target site at the 3′ untranslated region was confirmed by luciferase assay findings (Figure 4F). We then examined whether introduction of *miR-30d* or *miR-195* evoked a shift of the expression profile toward a cluster 2-like one (Figure 5A). Although both miRNAs were expressed at higher levels in cluster 2 than in cluster 1, introduction of either of the two miRNAs broadly affected the expression profiles, leading to decreased expression of genes that were expressed at higher levels in cluster 1 than in cluster 2 and *vice versa* (Figure 5A). Conversely, genes affected by introduction of *miR-30d* or *miR-195 in vitro* were found to be under differential influences of these miRNAs between tumors in clusters 1 and 2, showing that they had a significantly greater influence in cluster 2, which had higher expression of the two miRNAs than cluster 1 (Figure 5B and Supplementary Figure 4, available at *Carcinogenesis* Online).

Discussion

The present findings clearly demonstrate the existence of two major subtypes in lung adenocarcinomas based on their distinctive miRNA expression profiles. A group of tumors with high expression of developing lung-predominant miRNAs (cluster 1) including components of the *miR-17–92* cluster (15,16) were associated with aggressive growth, as manifested by prominent invasion and necrosis reflecting excessive proliferation, as well as poor prognosis after surgery. In marked contrast, the other major cluster (cluster 2) exhibited miRNA expression profiles similar to those of adult normal lung tissues and considerably retained normal lung characteristics such as the presence of TRU type and early phase of adenocarcinoma. Along this line, though the number of patients was small, those in subcluster 2a with expression profiles most reminiscent of adult normal lung tissues had no recurrence after surgery. Our previous finding of frequent downregulation of *let-7* in association with poor prognosis in lung cancer (10) may well correspond to the existence of tumors belonging to cluster 1, in which not only *let-7* but also other adult lung-predominant miRNAs with a gradual increase over the course of lung development were generally downregulated together, suggesting possible involvement of a coregulatory mechanism(s).

Our systems biology approach employing a Bayesian network and non-parametric regression allowed us to estimate the gene regulatory circuitry engaged in tumors of lung adenocarcinoma patients. A substantial proportion of the subnetworks identified as enriched for genes with differential expression between clusters 1 and 2 also exhibited enrichment of genes with proliferation-related functions, such as cell cycle and biomass production. This appears to be consistent with the finding that tumors in cluster 1 with poor prognosis exhibited both miRNA and mRNA expression profiles reminiscent of developing lungs, in which active cell proliferation takes place. In marked contrast, cluster 2 tumors with favorable prognosis showed resemblance to the expression profiles of adult lung tissues, which are populated with mostly quiescent epithelial cells (27). Thus, the present findings support the notion that lung adenocarcinomas can be divided into two major subtypes according to miRNA expression profiles, which seem to reflect either an actively proliferating developing lung-like biologic state or a well-committed adult lung-like state. Thus, it is possible that developmental machinery is involved in the acquisition of distinctive expression profiles and biologic features, warranting a future investigation to gain further insight into the driving force of that process.

The identified hub genes included two miRNAs, *miR-30d* and *miR-195*, and experimental evaluations clearly showed that

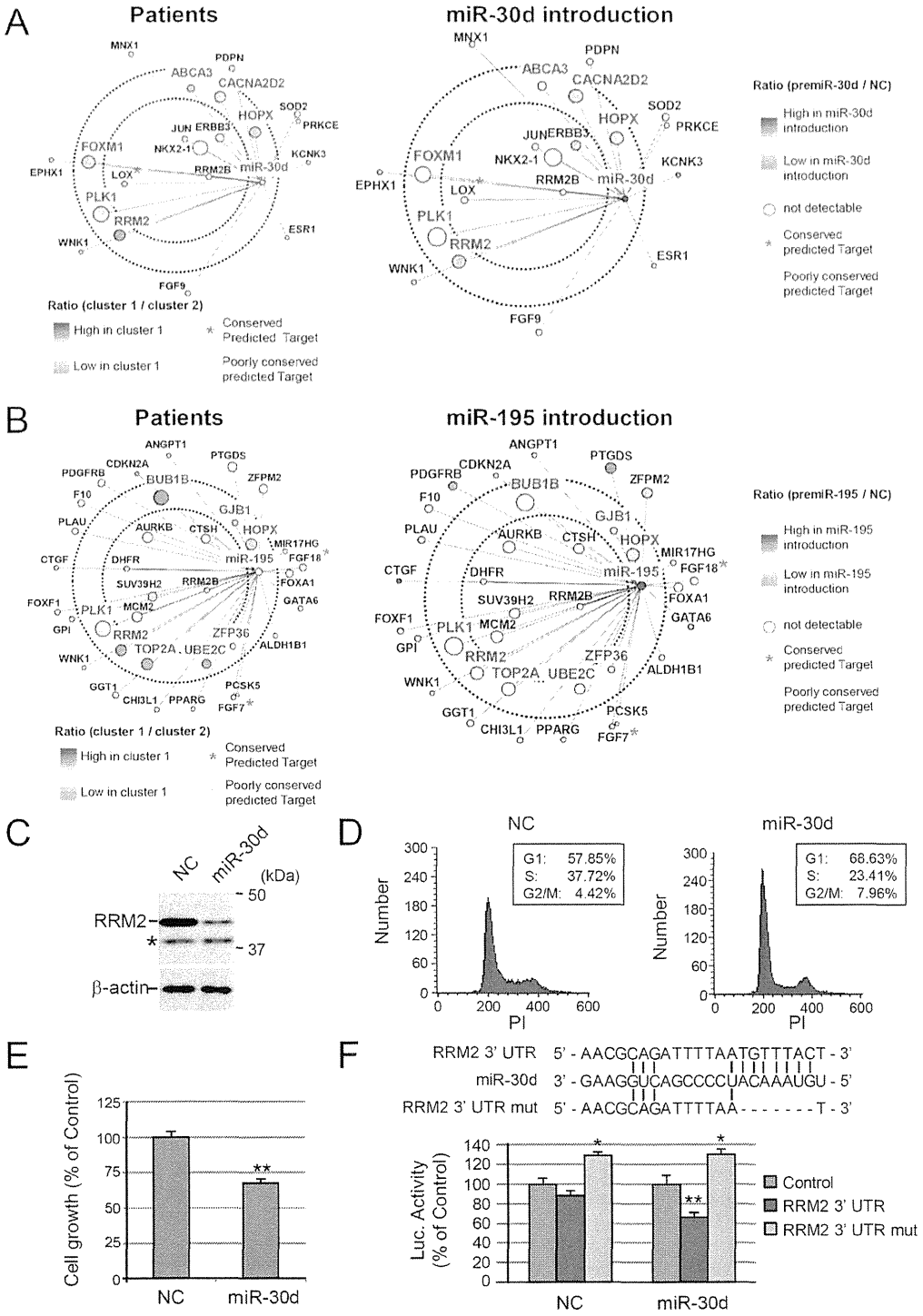

Fig. 4. Experimental evaluation of effects of hub miRNAs, *miR-30d*, and *miR-195*, on expression of their child genes. Shown are changes in expression of child genes of (**A**) *miR-30d* and (**B**) *miR-195* in SK-LC-7 cells treated with the corresponding miRNA mimics. (**C**) Western blotting, (**D**) flow cytometric, and (**E**) colorimetric analyses were performed using SK-LC-7 cells introduced with either *miR-30d* mimics or negative control (NC). (**F**) Luciferase assay findings obtained using reporter vector carrying either 3′ untranslated region of *RRM2* harboring potential *miR-30d* binding site or that with a 7-bp deletion corresponding to the seed sequence of *miR-30d*. $^*P < 0.05$; $^{**}P < 0.005$.

introduction of either one altered the mRNA expression profiles to resemble those of cluster 2, confirming their pivotal roles in the regulatory circuitry. Consistent with our experimental findings, we also observed that the regulatory influences of *miR-30d* and *miR-195* were more obvious in tumors belonging to cluster 2 than cluster 1, whereas these miRNAs were also expressed at higher levels in the former group. Thus, these miRNAs indeed appear to be engaged in tumors in gene regulation *in vivo*, which conceivably confers characteristic features of the miRNA expression profile-defined subtypes of lung adenocarcinomas. Our results also revealed that *miR-30d* directly targets *RRM2*, which was estimated to be a child gene in the *miR-30d*-centered subnetwork in

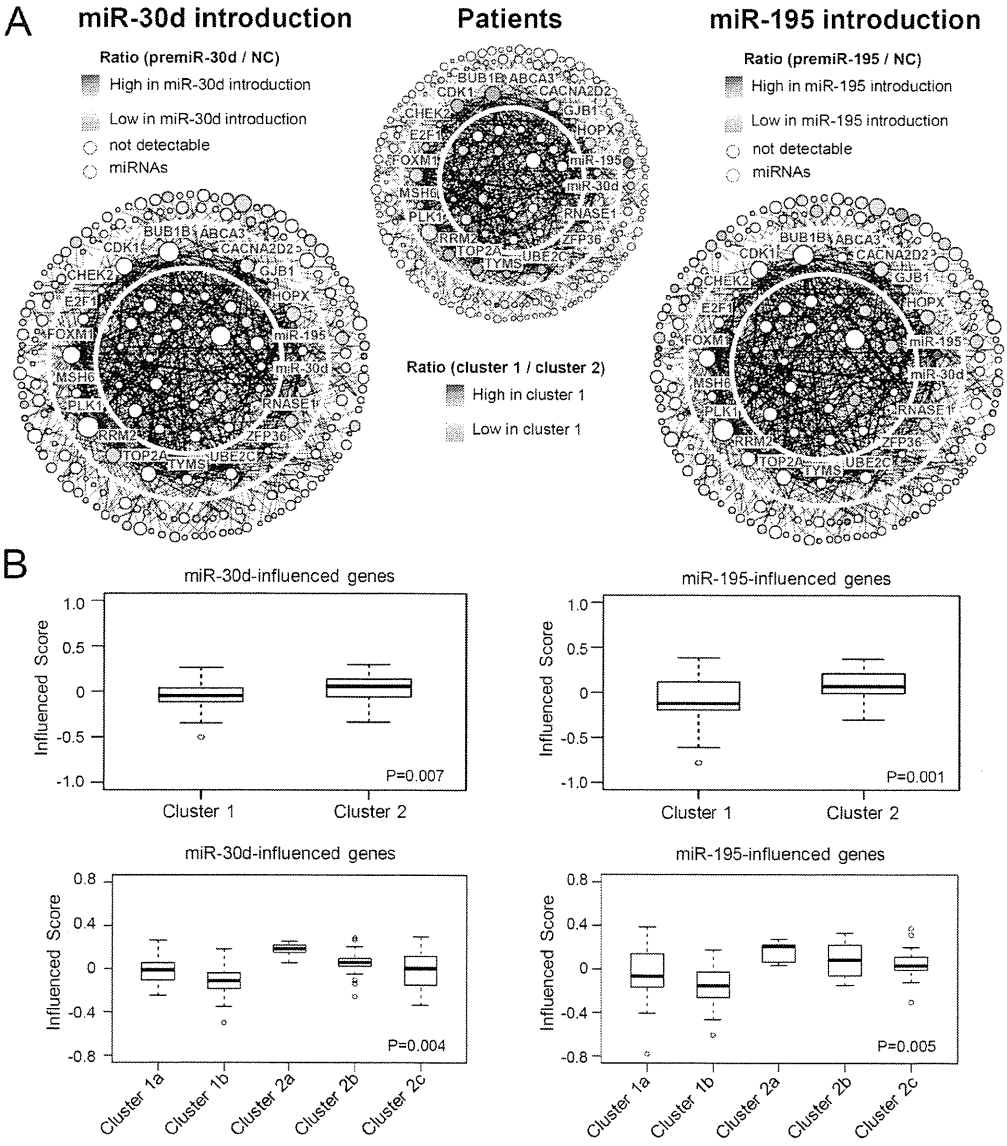

Fig. 5. Experimental and reverse *in silico* evaluations of effects of hub miRNAs, *miR-30d* and *miR-195*, on entire expression of the 19 subnetworks. (**A**) Changes in expression of all genes contained in the 19 subnetworks in SK-LC-7 cells treated with the corresponding miRNA mimics. (**B**) Reverse *in silico* evaluation of influences of miRNA expression in tumors from lung adenocarcinoma patients. Influence score: positive and negative values reflect changes in gene expression in experimentally observed and opposite directions, respectively. *P* values calculated using Wilcoxon rank sum and Kruskal–Wallis tests.

our network estimation. Reduced *miR-30d* and increased *RRM2* expression in cluster 1 appear to be consistent with a highly proliferative characteristic in association with worse prognosis, considering that RRM2 maintains a pool of deoxyribonucleotides for DNA replication and repair (28). We also noted that *RRM2B* encoding the p53-inducible subunit of ribonucleoreductase (29) was also placed as a child gene in the *miR-30d*-centered subnetwork, suggesting their possible regulatory relationship.

The present results show that lung adenocarcinomas can be classified into two major subtypes according to their miRNA expression profiles, each exhibiting resemblance to either developing or well-matured adult lungs in association with distinctive clinicopathologic features. Although an increasing number of miRNAs has been identified to have altered expression in various types of cancers, determination of their actual regulatory influences in tumors remains a challenge. In this regard, our study clearly demonstrates the usefulness of a robust systems biology approach, which may ultimately lead to elucidation of the entire picture of the altered regulatory circuitry involved in cancer development.

Supplementary material

Supplementary Materials and methods, Tables 1 and 2 and Figures 1–4 can be found at http://carcin.oxfordjournals.org/

Funding

Grants-in-Aid for Scientific Research on Innovative Areas from the Ministry of Education, Culture, Sports, Science and Technology (MEXT) of Japan (22134005 to T.T. and 22134004 to S.M.) and Grants-in-Aid for Scientific Research (A) (21249037 to T.T.) and Young Scientists (Start-up) from the Japan Society for the Promotion of Science (JSPS) (21890099 to C.A.).

Acknowledgements

We thank Y.Hosono and K.Cao for their technical suggestions and discussions.

Conflict of Interest Statement: None declared.

References

1. Travis,W.D. *et al.* (2011) International association for the study of lung cancer/American thoracic society/European respiratory society international multidisciplinary classification of lung adenocarcinoma. *J. Thorac. Oncol.*, **6**, 244–285.
2. Yamaguchi,T. *et al.* (2013) NKX2-1/TTF-1: an enigmatic oncogene that functions as a double-edged sword for cancer cell survival and progression. *Cancer Cell*, **23**, 718–723.
3. Yatabe,Y. *et al.* (2002) TTF-1 expression in pulmonary adenocarcinomas. *Am. J. Surg. Pathol.*, **26**, 767–773.
4. Tanaka,H. *et al.* (2007) Lineage-specific dependency of lung adenocarcinomas on the lung development regulator TTF-1. *Cancer Res.*, **67**, 6007–6011.
5. Takeuchi,T. *et al.* (2006) Expression profile-defined classification of lung adenocarcinoma shows close relationship with underlying major genetic changes and clinicopathologic behaviors. *J. Clin. Oncol.*, **24**, 1679–1688.
6. Yatabe,Y. *et al.* (2005) EGFR mutation is specific for terminal respiratory unit type adenocarcinoma. *Am. J. Surg. Pathol.*, **29**, 633–639.
7. Weir,B.A. *et al.* (2007) Characterizing the cancer genome in lung adenocarcinoma. *Nature*, **450**, 893–898.
8. Cancer Genome Atlas Research Network (2012) Comprehensive genomic characterization of squamous cell lung cancers. *Nature*, **489**, 519–525.
9. Osada,H. *et al.* (2007) MicroRNAs in biological processes and carcinogenesis. *Carcinogenesis*, **28**, 2–12.
10. Takamizawa,J. *et al.* (2004) Reduced expression of the let-7 microRNAs in human lung cancers in association with shortened postoperative survival. *Cancer Res.*, **64**, 3753–3756.
11. Hayashita,Y. *et al.* (2005) A polycistronic microRNA cluster, miR-17-92, is overexpressed in human lung cancers and enhances cell proliferation. *Cancer Res.*, **65**, 9628–9632.
12. Matsubara,H. *et al.* (2007) Apoptosis induction by antisense oligonucleotides against miR-17-5p and miR-20a in lung cancers overexpressing miR-17-92. *Oncogene*, **26**, 6099–6105.
13. Ebi,H. *et al.* (2009) Counterbalance between RB inactivation and miR-17-92 overexpression in reactive oxygen species and DNA damage induction in lung cancers. *Oncogene*, **28**, 3371–3379.
14. Taguchi,A. *et al.* (2008) Identification of hypoxia-inducible factor-1 alpha as a novel target for miR-17-92 microRNA cluster. *Cancer Res.*, **68**, 5540–5545.
15. Ventura,A. *et al.* (2008) Targeted deletion reveals essential and overlapping functions of the miR-17 through 92 family of miRNA clusters. *Cell*, **132**, 875–886.
16. Lu,Y. *et al.* (2007) Transgenic over-expression of the microRNA miR-17-92 cluster promotes proliferation and inhibits differentiation of lung epithelial progenitor cells. *Dev. Biol.*, **310**, 442–453.
17. Hanahan,D. *et al.* (2011) Hallmarks of cancer: the next generation. *Cell*, **144**, 646–674.
18. Lefebvre,C. *et al.* (2012) Reverse-engineering human regulatory networks. *Wiley Interdiscip. Rev. Syst. Biol. Med.*, **4**, 311–325.
19. Takahashi,T. *et al.* (1986) Two novel cell surface antigens on small cell lung carcinoma defined by mouse monoclonal antibodies NE-25 and PE-35. *Cancer Res.*, **46**, 4770–4775.
20. Ebi,H. *et al.* (2009) Relationship of deregulated signaling converging onto mTOR with prognosis and classification of lung adenocarcinoma shown by two independent in silico analyses. *Cancer Res.*, **69**, 4027–4035.
21. Tomida,S. *et al.* (2009) Relapse-related molecular signature in lung adenocarcinomas identifies patients with dismal prognosis. *J. Clin. Oncol.*, **27**, 2793–2799.
22. Eisen,M.B. *et al.* (1998) Cluster analysis and display of genome-wide expression patterns. *Proc. Natl Acad. Sci. U. S. A.*, **95**, 14863–14868.
23. Dong,J. *et al.* (2010) MicroRNA networks in mouse lung organogenesis. *PLoS One*, **5**, e10854.
24. Tamada,Y. *et al.* (2011) Sign: large-scale gene network estimation environment for high performance computing. *Genome Inform.*, **25**, 40–52.
25. Yamaguchi,T. *et al.* (2012) NKX2-1/TITF1/TTF-1-induced ROR1 is required to sustain EGFR survival signaling in lung adenocarcinoma. *Cancer Cell*, **21**, 348–361.
26. Nishikawa,E. *et al.* (2011) miR-375 is activated by ASH1 and inhibits YAP1 in a lineage-dependent manner in lung cancer. *Cancer Res.*, **71**, 6165–6173.
27. Morrisey,E.E. *et al.* (2010) Preparing for the first breath: genetic and cellular mechanisms in lung development. *Dev. Cell*, **18**, 8–23.
28. Nordlund,P. *et al.* (2006) Ribonucleotide reductases. *Annu. Rev. Biochem.*, **75**, 681–706.
29. Tanaka,H. *et al.* (2000) A ribonucleotide reductase gene involved in a p53-dependent cell-cycle checkpoint for DNA damage. *Nature*, **404**, 42–49.

Received November 22, 2013; revised May 30, 2014; accepted June 3, 2014

Oncogene (2015) **34,** 73–83

www.nature.com/onc

ORIGINAL ARTICLE

LIM-domain protein AJUBA suppresses malignant mesothelioma cell proliferation via Hippo signaling cascade

I Tanaka[1,2,6], H Osada[1,3], M Fujii[1], A Fukatsu[1,3], T Hida[4], Y Horio[4], Y Kondo[1], A Sato[5], Y Hasegawa[2], T Tsujimura[5] and Y Sekido[1,3]

Malignant mesothelioma (MM) is one of the most aggressive neoplasms usually associated with asbestos exposure and is highly refractory to current therapeutic modalities. MMs show frequent activation of a transcriptional coactivator Yes-associated protein (YAP), which is attributed to the neurofibromatosis type 2 (NF2)–Hippo pathway dysfunction, leading to deregulated cell proliferation and acquisition of a malignant phenotype. However, the whole mechanism of disordered YAP activation in MMs has not yet been well clarified. In the present study, we investigated various components of the NF2-Hippo pathway, and eventually found that MM cells frequently showed downregulation of LIM-domain protein AJUBA, a binding partner of large tumor suppressor type 2 (LATS2), which is one of the last-step kinases of the NF2-Hippo pathway. Although loss of AJUBA expression was independent of the alteration status of other Hippo pathway components, MM cell lines with AJUBA inactivation showed a more dephosphorylated (activated) level of YAP. Immunohistochemical analysis showed frequent downregulation of AJUBA in primary MMs, which was associated with YAP constitutive activation. We found that AJUBA transduction into MM cells significantly suppressed promoter activities of YAP-target genes, and the suppression of YAP activity by AJUBA was remarkably canceled by knockdown of LATS2. In connection with these results, transduction of AJUBA-expressing lentivirus significantly inhibited the proliferation and anchorage-independent growth of the MM cells that harbored ordinary LATS family expression. Taken together, our findings indicate that AJUBA negatively regulates YAP activity through the LATS family, and inactivation of AJUBA is a novel key mechanism in MM cell proliferation.

Oncogene (2015) **34,** 73–83; doi:10.1038/onc.2013.528; published online 16 December 2013

Keywords: malignant mesothelioma; Hippo pathway; YAP; AJUBA; LATS2

INTRODUCTION

Malignant mesothelioma (MM), which arises from mesothelial cells, is a highly aggressive human malignancy.[1,2] Global mesothelioma deaths were reported to be about 100 000 in 83 countries by the World Health Organization between 1994 and 2008.[3] MM mortality rates are estimated to increase by 5–10% per year in most industrialized countries until about 2020.[4] Despite intensive treatment with chemotherapy, radiation therapy or surgery, the disease carries a poor prognosis. The median survival time of patients after diagnosis is only 7–12 months.[5–7] MM is usually caused by asbestos exposure, and the latency period after initial exposure is typically longer than 30 years,[8] which connotes accumulation of multiple genetic and epigenetic alterations for MM development.[9] However, the exact molecular pathological process of the development and progression of MM remains obscure.

Around 50% of MM tumors have a genetic mutation of the neurofibromatosis type 2 (*NF2*) tumor suppressor gene.[10,11] *NF2* encodes merlin, a member of the ezrin/radixin/moesin protein family. Merlin is an upstream regulator of the Hippo signaling cascade, which is conserved from *Drosophila* to mammalians.[12,13] The Hippo signaling pathway controls organ size through the regulation of cell cycle, proliferation and apoptosis.[14,15] The mammalian components of this pathway include WW domain-containing protein 1 (WWC1, also called KIBRA), Serine/threonine protein kinase 3 and 4 (STK3 and 4, also called MST2 and 1, orthologs of *Drosophila* Hippo), SAV1, and serine/threonine kinase large tumor suppressor 1 and 2 (LATS1 and 2). Activation of the NF2–Hippo pathway induces the activation of LATS1/2, which phosphorylates and inactivates a transcriptional coactivator, Yes-associated protein (YAP), by translocating YAP from the nucleus to the cytoplasm. The dysfunction of the Hippo pathway, which leads to increased YAP activity with an underphosphorylated form in the nucleus, induces oncogenic transformation owing to activation of transcription factors including TEAD family members.[16] Several target genes of the YAP/TEAD transcriptional complex, including connective tissue growth factor (*CTGF*) and *CCND1* genes, have been shown to be responsible for tumor progression.[12,17,18] We previously reported frequent YAP activation (underphosphorylation) in more than 70% of primary MMs and its pro-oncogenic role in MM cells.[19,20] Besides *NF2* mutation, we also found that a subset of MM tumors harbors inactivating mutations of *LATS2* and *SAV1*.[20] Nevertheless, some MM cases without any of these gene alterations still displayed YAP activation, leading us to hypothesize that the other components related to the Hippo pathway might be altered in these cases.

AJUBA family proteins (AJUBA, LIMD1 and WTIP) belong to the Zyxin/AJUBA family, which are components of both

[1]Department of Thoracic Oncology Oncology, Aichi Cancer Center Research Institute, Nagoya, Japan; [2]Department of Respiratory Medicine, Nagoya University Graduate School of Medicine, Nagoya, Japan; [3]Department of Cancer Genetics, Program in Function Construction Medicine, Nagoya University Graduate School of Medicine, Nagoya, Japan; [4]Department of Thoracic Oncology, Aichi Cancer Center Hospital, Nagoya, Japan and [5]Department of Pathology, Hyogo College of Medicine, Nishinomiya, Japan. Correspondence: Dr Y Sekido, Division of Molecular Oncology, Aichi Cancer Center Research Institute, Kanokoden 1-1, Chikusa-ku, Nagoya, Aichi 464-8681, Japan.
E-mail: ysekido@aichi-cc.jp
[6]Awardee of Research Resident Fellowship from the Foundation for Promotion of Cancer Research.
Received 4 June 2013; Received 22 October 2013; accepted 25 October 2013; published online 16 December 2013

integrin-mediated and cell–cell junction adhesive complexes in the capacity of adaptor or scaffold protein.[21] These adaptor or scaffold proteins are known to be crucial regulators of many key signaling pathways, which are involved in cell–cell adhesion, actin cytoskeleton modulation, mitosis, repression of gene transcription, cell differentiation, proliferation and migration.[22,23] Although the mechanisms have not yet been strictly defined, the regulation of their signal pathways is known to be executed by assisting proper localization of signaling components, which include interacting and/or binding with multiple members of signaling pathways, tethering them into complexes.[24,25] In this regard, AJUBA family proteins have been identified to be a binding partner of the LATS family, and the LATS2–AJUBA complex regulates γ-tubulin recruitments involved in mitosis.[26] Recently, Jub (*Drosophila* ortholog of AJUBA family proteins) was shown to activate yorki (*Drosophila ortholog of* YAP) through suppression of the Hippo pathway, and AJUBA family proteins were also found to inhibit YAP phosphorylation in HEK293 and MDCK cells.[27] AJUBA family proteins are thought to be involved in distinct signaling cascades as a multifunctional protein. These studies lead us to hypothesize that AJUBA family proteins might be one of the crucial factors involved in the dysregulation of the Hippo signaling pathway in MM cells.

In this study, using MM cell lines and primary tumors we found that MMs have frequent downregulation of AJUBA, besides the *NF2*, *LATS2* and/or *SAV1* inactivation shown in our previous report.[20] We also found that AJUBA negatively regulates YAP activity through LATS1/2 in MM cells.

RESULTS

Frequent reduction of AJUBA expression in MM cell lines

In our previous study, we reported that most MM cell lines harbored either one or two of the *NF2, LATS2* and/or *SAV1* gene mutations, which encode major components of the Hippo signaling pathway.[20] The inactivation of these genes leads to the aberrant activation of YAP through decreased phosphorylation of YAP (S127) and more malignant phenotypes of cells.[20] However, there were several MM cell lines that showed YAP activation (underphosphorylation) despite the absence of any of these gene mutations. To determine whether the Hippo signaling pathway inactivation can be caused by alteration of other components, we expanded the analysis of the Hippo signaling pathway including other members in this cascade. Using a panel of 19 of 24 MM cell lines that we previously described[20] and 5 newly established cell lines, we examined the expression status of seven proteins including AJUBA, LIMD1, WTIP, MST1, MST2, LATS1 and KIBRA, which were not characterized in our previous study (Figure 1a and Supplementary Figure S1a). We also reanalyzed the expressions of Merlin, SAV1, LATS2 and YAP, and the phosphorylation status of YAP (S127) (Figure 1a and Supplementary Figure S1a), and confirmed our previous data.[18,20] Although the phosphorylation status of YAP (S127) was different in several cell lines from the previous study, possibly because of the different culture conditions, the overall underphosphorylation status of YAP was consistent, with 21 (85%) of 24 MM cell lines showing YAP activation (Figure 1b).

Interestingly, the expression of AJUBA was significantly reduced in 18 of 24 (75%) MM cell lines (Figure 1a). All six cell lines with intact *NF2, SAV1* and *LATS1/2*, including NCI-H28, -H2452, Y-MESO-29, -48, -72 and ACC-MESO-4, showed the downregulation of AJUBA, and four of the six cell lines showed activation (underphosphorylation) of YAP (Supplementary Table 1). Meanwhile, low expression of AJUBA was also observed in 11 of 15 MM cell lines with *NF2* inactivation, and the YAP phosphorylation levels tended to be more reduced in 11 cell lines with AJUBA downregulation (Supplementary Figures S1b and S1c, black columns) compared with four cell lines that retained AJUBA expression (white columns), although the difference was not statistically significant ($P = 0.057$). These results suggested that AJUBA might modulate Hippo signaling while affecting YAP phosphorylation status, and that the alteration of AJUBA expression might be involved in the tumorigenic process of MM. On the other hand, the expression levels of MST1/2 were not decreased in all MM cell lines, and LIMD1, LATS1 and KIBRA were markedly reduced in only three, four and two cell lines, respectively (Figure 1a and Supplementary Figure S1a).

To determine whether AJUBA reduction was caused at the transcriptional level, we carried out real-time reverse transcription–PCR analysis of *AJUBA* together with *WTIP, MST1* and *LATS1* (Supplementary Figure S2). Several cell lines with low AJUBA protein expression, including Y-MESO-8D and Y-MESO-29, displayed low *AJUBA* mRNA expressions. However, other low AJUBA protein-expressing cell lines such as ACC-MESO-4 and Y-MESO-9 did not show *AJUBA* mRNA downregulation. These results suggested that the reduction of AJUBA in MM cells is induced either at the transcriptional or at the post-transcriptional levels.

Regarding WTIP, several cell lines showed relatively weak WTIP expression in western blot analysis, but, due to a possible low specificity of the antibody (discussed below in Supplementary Figure S3), we also conducted real-time reverse transcription–PCR analysis and found several cell lines with low expressers of *WTIP* (Supplementary Figure S2).

AJUBA is associated with increased YAP phosphorylation in MM cells

To determine whether AJUBA downregulation is involved in the Hippo signaling dysregulation in MM cells, we studied three MM cell lines with low AJUBA expression, including NCI-H290, Y-MESO-8D and NCI-H28 (Supplementary Table 1, indicated in pink in the cell line names). NCI-H290 and Y-MESO-8D cell lines with *NF2* mutation showed YAP activation (underphosphorylation), whereas the other components of the Hippo pathway were intact. NCI-H28 had intact NF2 and the Hippo pathways, but YAP phosphorylation was moderately activated.

Using these cell lines with low AJUBA expression, we transduced AJUBA-expressing lentivirus and studied the changes in YAP phosphorylation status. Surprisingly, we found that exogenous AJUBA markedly led to an increase in YAP phosphorylation levels in all three cell lines (Figures 2a and b), which seemed to be contrary to the result in the previous report on *Drosophila*—that is, dJub dephosphorylates Yorkie.[27] To exclude a possibility that ectopically expressed AJUBA was too abundant and caused this unexpected result, we also compared AJUBA overexpression levels in the three AJUBA-transduced cell lines with endogenous AJUBA expression levels in MeT-5A, and in two AJUBA-unsuppressed MM cell lines, MSTO-211H and Y-MESO-43 (Supplementary Figures S2b and S2c). We found that the transduced AJUBA expression levels were about threefold higher than the endogenous basal levels, which seemed to be acceptable levels for *in vitro* functional assays.

To confirm whether or not YAP phosphorylation induced by AJUBA transduction affects the expression of transcriptional targets of YAP, we studied *CCND1*, one of the YAP-target genes, and found a decrease in CCDN1 protein expression in all three cell lines (Figure 2a). Furthermore, dual-luciferase assay using the promoter reporters of the *CCND1* and *CTGF* genes, the latter being another known YAP target,[18] clearly demonstrated that exogenous AJUBA markedly suppressed both promoter activities (Figures 2c and d). Conversely, RNA interference-mediated silencing of endogenous AJUBA led to the decrease in YAP phosphorylation levels in MeT-5A and Y-MESO-43 cells with ordinary expression of all three AJUBA family proteins (Supplementary Figures S3a and S3b). Likewise, AJUBA small interfering RNA transduction in MeT-5A cells increased both *CCND1* and *CTGF* promoter activities, indicating that

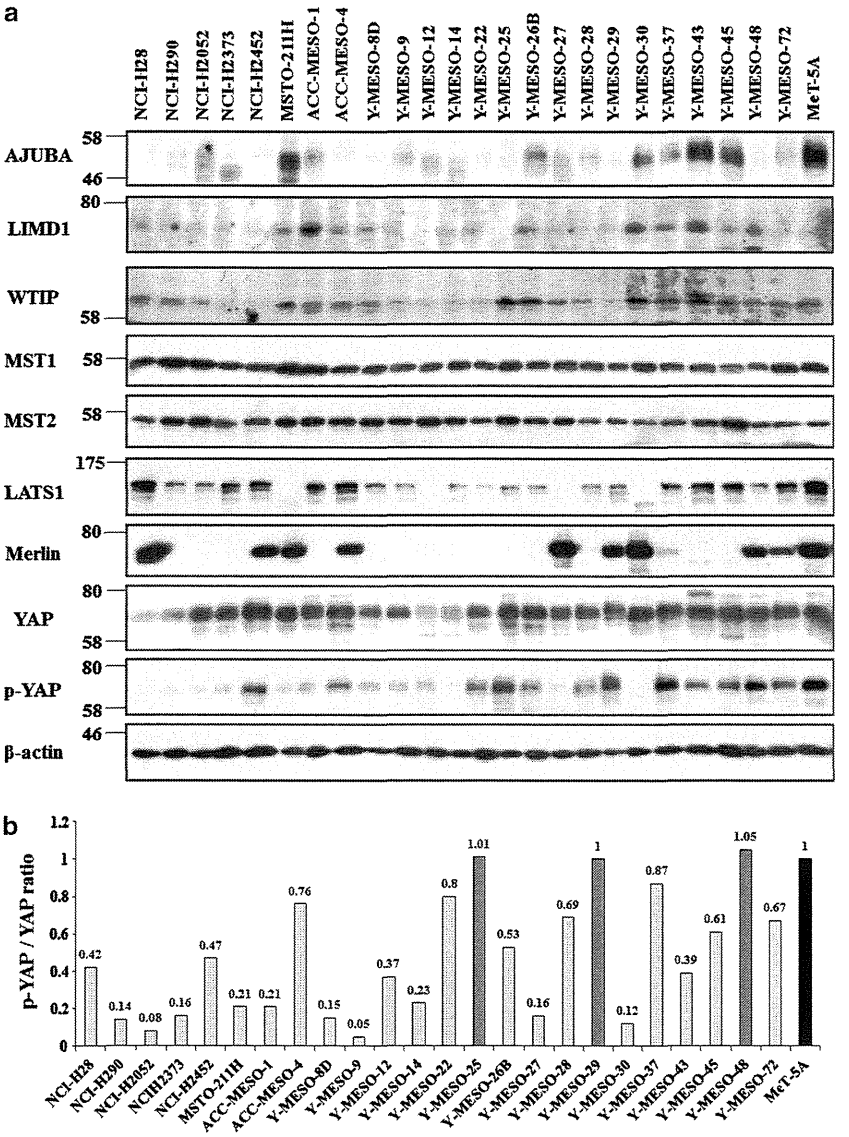

Figure 1. Expression analysis of the Hippo pathway components in MM cell lines. (**a**) Western blot analysis of AJUBA, LIMD1, WTIP, MST1, MST2, LATS1, Merlin, YAP and phospho-YAP Ser127 (p-YAP). AJUBA expression was undetectable in 15 and significantly low in 3 of 24 MM cell lines compared with an immortalized normal mesothelial cell line MeT-5A (also see Supplementary Table 1). Expression levels of LIMD1 or LATS1 were significantly reduced in 3 or 4 MM cell lines, respectively. No reduction of MST1 and MST2 was observed in any MM cell line. Merlin (*NF2* gene product) expression was undetectable in 14 and significantly low in one of 24 MM cell lines, compared with MeT-5A cells. YAP phosphorylation level was remarkably reduced in 21 of 24 MM cell lines compared with MeT-5A. Expression of β-actin was used as the control. (**b**) p-YAP and YAP signals shown in **a** were measured and the intensity ratios were shown with a bar graph with reference to MeT-5A. Lower p-YAP/YAP value indicates higher YAP activation status.

endogenous AJUBA also regulates YAP-target gene transcription (Supplementary Figure S3c). In contrast, silencing of endogenous WTIP increased YAP phosphorylation levels in both MeT-5A and Y-MESO-43 cells (Supplementary Figures S3a and S3b). Expression of WTIP small interfering RNA was also assessed at the mRNA level, because western blot analysis did not sufficiently confirm the effect of small interfering RNA knockdown (Supplementary Figure S3d).

AJUBA indirectly induces YAP phosphorylation via the LATS family

To determine whether YAP phosphorylation induced by AJUBA transduction is dependent on the Hippo signaling cascade, we transduced AJUBA into two MM cell lines, Y-MESO-14 and Y-MESO-27, which harbored *LATS2* homozygous deletion.[20] As YAP is directly phosphorylated by LATS1 or LATS2, and these two cell lines showed different LATS1 status (Y-MESO-14 had it, but Y-MESO-27 had lost LATS1 expression), we considered that these cell lines were useful for vigorous examination of a possible LATS family effect on AJUBA (Figure 3a).

After AJUBA transduction, the YAP phosphorylation level was slightly increased in Y-MESO-14 cells with LATS1 expression, whereas Y-MESO-27 cells without LATS1 expression did not show any change in the YAP phosphorylation level (Figures 3a and b). The dual-luciferase reporter assay also confirmed that AJUBA transduction suppressed neither the activity of *CCND1* nor that of the *CTGF* promoter in Y-MESO-27 cells (Figure 3c). These results indicated that AJUBA induces YAP phosphorylation via LATS1/2 in MM cells.

To further confirm these results, we conducted knockdown of LATS1 or LATS2 in NCI-H290 and Y-MESO-8D cell lines, both having intact LATS1/2, after infection of AJUBA-expressing lentivirus. Interestingly, LATS2 knockdown significantly suppressed YAP phosphorylation induced by exogenous AJUBA in both cell lines,

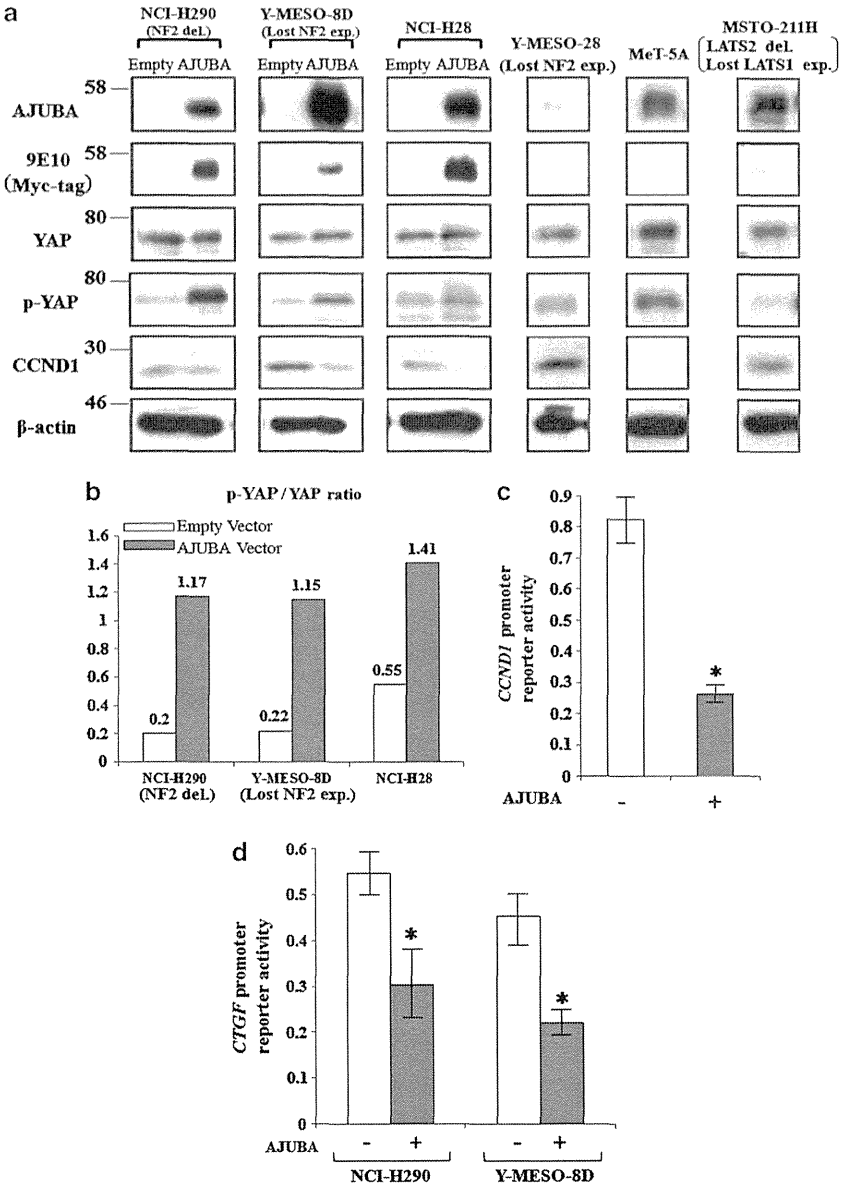

Figure 2. AJUBA is associated with an increased YAP phosphorylation level. (**a**) Western blot analyses. NCI-H290, Y-MESO-8D and NCI-H28 cells were infected with AJUBA-expressing or empty lentivirus. AJUBA transduction led to a marked increase in YAP phosphorylation levels and to a decrease in CCND1 expression levels in these three cell lines. Ectopically expressed AJUBA and subsequent effects on YAP and CCDN1 were compared with the patterns in another three cell lines.Y-MESO-28, another representative AJUBA-low cell line, showed a phospho-YAP-low and CCND1-high pattern, whereas MeT-5A expressing ordinary level of AJUBA showed a phospho-YAP-high and CCND1-low pattern; these patterns were similar to the results of empty and AJUBA transduction in the three cell lines. Meanwhile, MSTO-211H also expressed AJUBA as abundantly as MeT-5A, but showed high-CCND1 expression compared with MeT-5A, because of its *LATS2* deletion and low-LATS1 expression. (**b**) p-YAP and YAP signals shown in **a** were measured, and the intensity ratios were indicated with a bar graph. (**c**) *CCND1* promoter reporter assay. *CCND1* promoter reporter construct was transfected into NCI-H290 cells together with an AJUBA-expressing vector, pcDNA3-AJUBA, or empty vector. AJUBA markedly suppressed the *CCND1* promoter activity. (**d**) *CTGF* promoter reporter assay. *CTGF* promoter reporter construct was transfected into NCI-H290 and Y-MESO-8D cells together with pcDNA3-AJUBA, or empty vector. AJUBA significantly suppressed the *CTGF* promoter activity in both cell lines. Average and s.d. of triplicated experiments are demonstrated in **c** and **d**. *$P<0.05$ versus empty vector control. del., deletion; exp., expression.

whereas LATS1 knockdown showed only moderate suppression (Figures 3d and e). Furthermore, dual-luciferase assays showed that LATS2 knockdown in NCI-H290 cells effectively recovered the *CCND1* promoter activity that was suppressed by AJUBA (Figure 3f). Similarly, LATS2 knockdown effectively recovered the *CTGF* promoter activity that was attenuated by AJUBA, whereas LATS1 knockdown showed only a marginal effect (Figure 3g and Supplementary Figure S3e). These results indicated that AJUBA led to increased YAP phosphorylation and inhibited the transcriptional coactivity of YAP through the LATS family, and that its effect seemed to be relatively more dependent on LATS2 than on LATS1.

AJUBA mainly localizes in the MM cell cytoplasm and translocates YAP

YAP, when phosphorylated, is known to translocate from the nucleus to the cytoplasm.[28] To investigate whether AJUBA is also

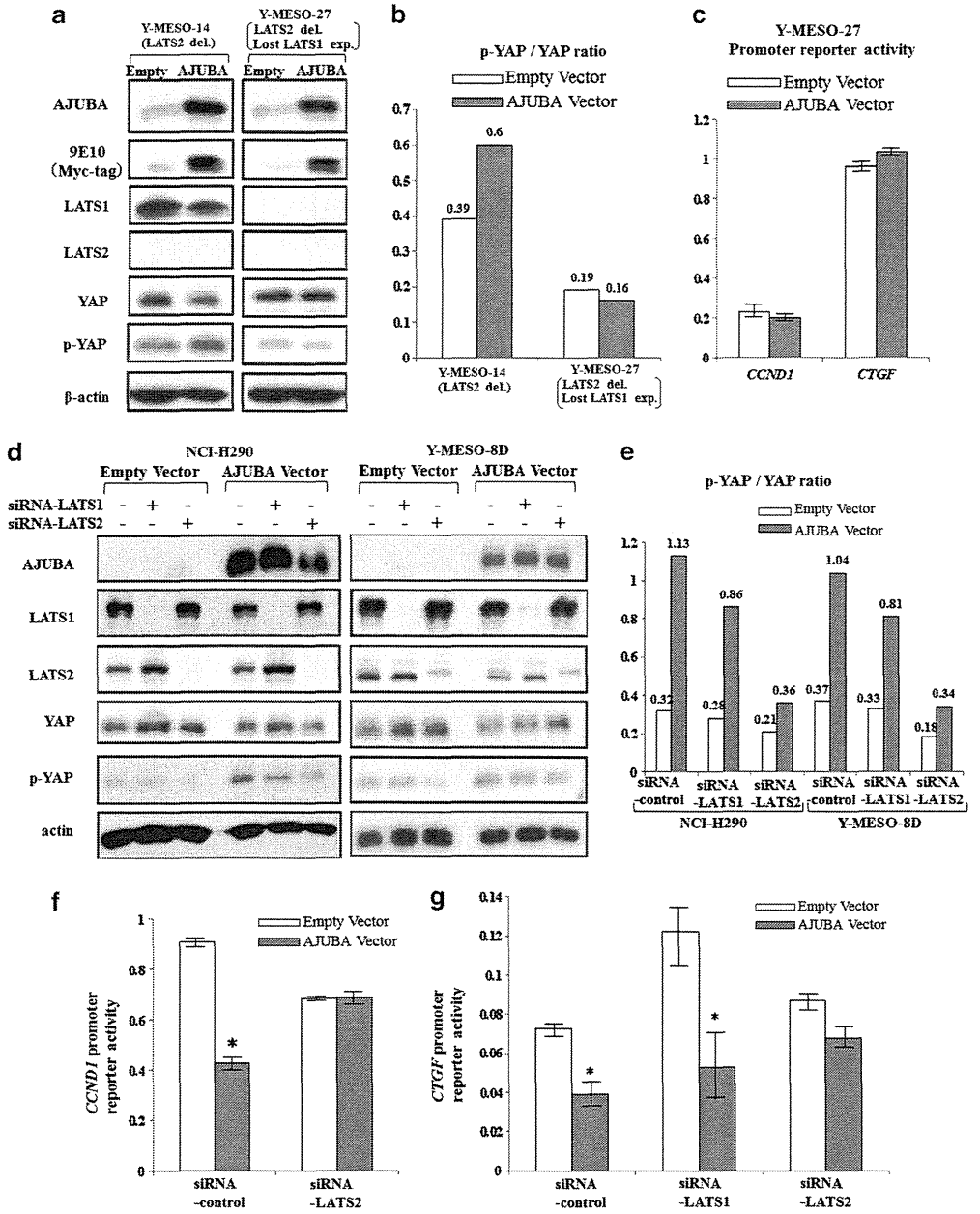

Figure 3. AJUBA indirectly increases YAP phosphorylation level through LATS family. (**a**) Y-MESO-14 and Y-MESO-27 cells harboring *LATS2* homozygous deletion were infected with Myc-tagged AJUBA-expressing or empty lentivirus. Western blot analysis demonstrated that exogenous AJUBA led to a slight increase in the YAP phosphorylation level in Y-MESO-14 cells with ordinary LATS1 expression, but not in Y-MESO-27 cells, which had simultaneous downregulation of LATS1. (**b**) p-YAP and YAP signals presented in **a** were measured and indicated with a bar graph as p-YAP/YAP ratio. (**c**) Promoter reporter assays. *CCND1* or *CTGF* promoter reporter construct was transfected into Y-MESO-27 cells with both LATS1 and LATS2 inactivation. AJUBA co-transduction did not affect either of the two promoter activities. (**d**) After infection of AJUBA-expressing or empty lentivirus, small interfering RNA-induced knockdown of LATS1 or LATS2 was conducted using NCI-H290 and Y-MESO-8D cells. LATS2 knockdown effectively, but LATS1 knockdown only slightly, suppressed phospho-YAP levels, despite AJUBA transduction. (**e**) p-YAP and YAP signals shown in **d** are indicated with a bar graph of p-YAP/YAP ratio. (**f**) *CCND1* promoter reporter assay using NCI-H290 cells. After transfection of the *CCND1* promoter reporter together with AJUBA-expressing vector (or empty vector), small interfering RNA against LATS2 was transfected, and then dual-luciferase reporter assay was conducted. Suppression of *CCND1* promoter activity by AJUBA was canceled by LATS2 knockdown. (**g**) *CTGF* promoter reporter assay. After transfection of the *CTGF* promoter reporter with AJUBA-expressing vector (or empty vector) into Y-MESO-8D cells, the small interfering RNA against LATS1 or LATS2 was transfected, and then dual-luciferase reporter assay was conducted. AJUBA markedly suppressed the activity of *CTGF* promoter, and LATS2 knockdown effectively, but LATS1 knockdown only marginally, attenuated the suppression of *CTGF* promoter activity by AJUBA. Average and s.d. of triplicated experiments are demonstrated in **c**, **f** and **g**. $^*P<0.05$ versus small interfering RNA control.

associated with YAP translocation in MM cells, we performed a cell fractionation experiment using two MM cell lines after AJUBA transduction. Western blot analysis of nuclear and cytoplasmic fractions of the transfectants showed that exogenous AJUBA was mainly expressed in the cytoplasmic fraction and that YAP and phospho-YAP (Ser127) levels were significantly increased in the cytoplasm in both cell lines (Figures 4a and b).

Next, we performed immunofluorescent analysis to confirm the subcellular localization for exogenously expressed AJUBA in Y-MESO-8D cells and for endogenous AJUBA in MeT-5A cells. The results